Complex Signal Processing is Not — Complex

Ken Martin
martin@eecg.toronto.edu
Dept. of Elect. and Comp. Engr., Univ. of Toronto,
Toronto, ON Canada M5S 3G4

Abstract: Wireless systems often make use of the quadrature relationship between pairs of signals to effectively cancel out-of-band and interfering in-band signal components. The understanding of these systems is often simplified by considering both the signals and system transfer-functions as *'complex'* quantities. The complex approach is especially useful in highly-integrated multi-standard receivers where the use of narrow-band fixed-coefficient filters at the RF and high IF frequencies must be minimized. A tutorial review of complex signal processing for wireless applications emphasizing a graphical and pictorial description rather than an equation-based approach is first presented. Next, a number of classical modulation architectures are described using this formulation. Finally, more recent developments such as complex filters, image-reject mixers, low-IF receivers, and over-sampling A/D converters are discussed.

1. Introduction

A *complex* signal consists of a pair of *real* signals at an instance in time. If one denotes the complex signal, $X(t)$, as $X(t) = x_r(t) + jx_q(t)$, where $j = \sqrt{-1}$, then a Hilbert Space can be defined using appropriate definitions for addition, multiplication, and an inner-product and norm. In an actual physical system, the signals are both real (but are called the real and imaginary parts) and are found in two distinct signal paths. The multiplier 'j' is used to help define operations between different complex signals, and is to some degree *imaginary*, i.e., it doesn't actually exist in real systems. Often the dependence of signals on time is not shown explicitly.

The use of *complex* signal processing to describe wireless systems is increasingly important and ubiquitous for the following reasons: it often allows for image-reject architectures to be described more compactly and simply, it leads to a graphical or *signal-flow-graph* (SFG) description of signal-processing systems that gives insight, and it often leads to the development of new systems where the use of high-frequency, highly selective image-reject filters is minimized leading to more highly integrated transceivers using less power and requiring less physical space.

As an example, consider the popular '*image-reject*' mixer having a *real* input as shown in Fig. 1. In the complex SFG, two real multiplications have been replaced by a single complex multiplication. Furthermore, since in the time domain we have

$$Y(t) = y_r(t) + jy_q(t) = X(t)e^{j\omega_i t} \quad (1)$$

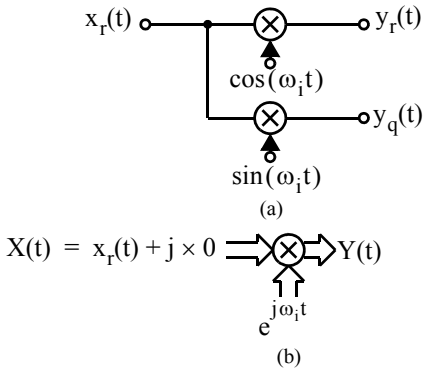

Fig. 1. A signal-flow-graph (SFG) of an image-reject mixer using (a) a real SFG and (b) a complex SFG.

then taking the Fourier Transform we have

$$Y(\omega) = X(\omega - \omega_i) \quad (2)$$

and we see that an ideal image-reject mixer results in a simple frequency-shift of the input signal with no images occurring, a conclusion that is obvious from Fig. 1. (b), but is certainly not obvious from Fig. 1. (a).

The use of complex signal processing for wireless applications has blossomed recently. This is especially true for high-bit-rate standards, such as local-area-networks (LAN's), and for multi-standard transceivers. Evidence of this proliferation is that in 2001, 2002, and 2003, the *majority* of the papers in *IEEE ISSCC* sessions on wireless transceivers for LAN applications employed complex signal processing.

Much, but not all, of this paper deals with a tutorial review of complex signal processing, especially as applicable to wireless systems. A great deal of the tutorial material on complex *analog* signal processing is directly based on the pioneering research of W. Martin Snelgrove as described in [1][6][7], and in some theses of his graduate students in [9] and [11]. Unfortunately, no journal publications of this early work were published[1]. Some of the early published work on complex digital filters is described in [2] and [5]. It is speculated that the development of complex filters was partially due to the use of Fortran to simulate and design filters and the fact that Fortran could do complex math — an example of a solution finding a problem.

This paper starts with a review of the fundamentals of complex signal processing. Some important identities are given. Examples are given using complex SFG representations. In the

1. A paper was submitted to the *IEEE Transactions on Circuits and Systems*, in 1981, but it was inexplicably rejected; a copy of this key paper submission has been obtained and is available at [8].

third section, a number of classical wireless modulations systems are described using the complex formulation. These systems include Weaver and Hartley modulators and polyphase filters. Errors due to non-ideal coefficients in mixers are quantified. In the fourth section, complex analog and digital filters are discussed. The fifth section describes more-recent complex signal-processing applications. These include complex adaptive image-reject mixers, complex low-IF receiver architectures including a new modulation approach that doubles the data rate for a given A/D sampling frequency, and complex band-pass over-sampling A/D converters, as examples. These systems are especially useful in multi-standard wireless applications as they are inherently wide-band (without excessive imaging errors) and allow the systems to be adapted to individual standards using digital programming after the A/D converters.

2. Complex Signal Processing

Complex signal processing systems operate on ordered-pairs of real signals. The typical definition of a complex inner-product is

$$\langle x_1(t), x_2(t)\rangle = \lim_{t\to\infty}\frac{1}{2t}\int_{-t}^{t} x_1(\tau)x_2^*(\tau)d\tau \qquad (3)$$

Combining this definition with the typical definitions for complex inversion, addition and multiplication, and the properties of commutation and association, constitutes a Hilbert Space. It is assumed that all signals are effectively of finite-energy and frequency and time limited (or periodic). This implies that a signal, $x_i(t)$ can be represented as a finite series of *complexoids*[2]

$$x_i(t) = \sum_{i=-N}^{N} k_i e^{j\omega_0 it} \qquad (4)$$

where k_i is in general complex [5]. In this paper, we will limit our consideration normally to a single (or a few) complexoids to simplify explanations. The generalization to signals as defined by (4) is left for a later date.

2.1 Complex Operations

A complex addition of two complex signals simply adds the two real parts and the two imaginary parts independently. Consider the real SFG that represents adding a complex signal to a second complex signal as shown in Fig. 2. (a). Its complex SFG is shown in Fig. 2. (b).

Slightly more complicated is a complex multiplication; consider multiplying a complexoid $X(t) = e^{j\omega_i t}$ by a complex coefficient $K = a + jb$. We have

$$Y(t) = \{a\cos(\omega_i t) - b\sin(\omega_i t)\} + j\{a\sin(\omega_i t) + b\cos(\omega_i t)\} \qquad (5)$$

The real SFG of this operation is shown in Fig. 3. (a). Once again the complex SFG of a multiplication operation, as shown in Fig. 3. (b), is considerably simpler. Note that the real SFG does not include the constant j anywhere, whereas in the complex SFG, it is admissible.

2. Historically, a *complexoid* had been called a *cissoid*. The author prefers the former name.

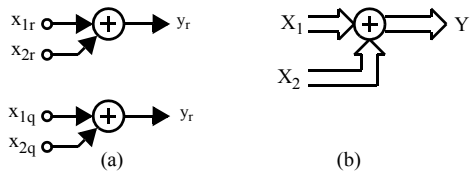

Fig. 2. (a) The real SFG for adding two complex signals and (b) the equivalent complex SFG.

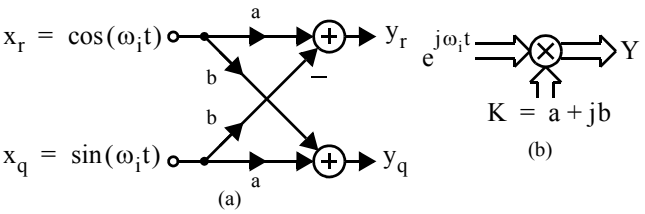

Fig. 3. (a) The real SFG of a complex multiply and (b) the equivalent complex SFG.

A special case of multiplication is when multiplying an input signal by the constant j. This is shown using a complex SFG in Fig. 4. (a) and a real SFG in Fig. 4. (b). It is seen this operation is simply an interchanging of the real and inverted imaginary parts; this operation is the basis behind realizing imaginary components in complex networks.

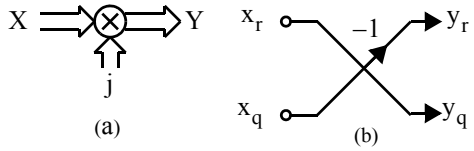

Fig. 4. Multiplying a signal by j.

Another important operation is complex conjugation. Consider

$$X(t) = Me^{j\phi}e^{j\omega_i t} \qquad (6)$$

We have

$$X^*(t) = Me^{-j\phi}e^{-j\omega_i t} \qquad (7)$$

and we see that besides being phase rotated, X has been transformed from a positive frequency into a negative frequency complexoid. Conjugation also changes negative frequencies complexoids to positive frequencies. The conjugation operation is shown in the real SFG of Fig. 5. (a). Alternative complex SFG's are shown in Fig. 5. (b) and (c).

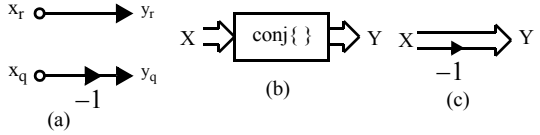

Fig. 5. The complex conjugation operation.

Two additional operations are required for realizing complex filters, namely the delay operator for digital filters and the integration operator for analog filters. These operations simply consist of independently applying the real operation to each part of the complex signal as shown in Fig. 6.

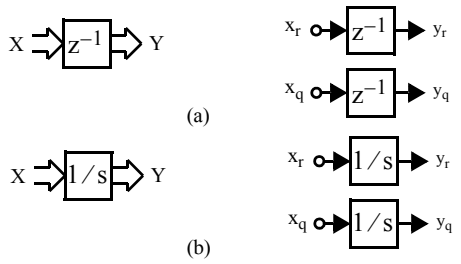

Fig. 6. (a) The digital delay operator and (b) the analog integration operator for complex signals.

2.2 Polar to Rectangular Conversion

Complex signals at a single frequency, possibly positive, possibly negative, or possibly both, can be expressed in either polar or rectangular form. In polar form we have

$$X(t) = Pe^{j\omega_i t} + Ne^{-j\omega_i t} \tag{8}$$

where P and N are possibly complex coefficients. Alternatively, we can express $X(t)$ in rectangular form as

$$X(t) = A\cos(\omega_i t) + jB\sin(\omega_i t) \tag{9}$$

It is straight-forward to show P, N are related to A, B using the duality

$$\begin{aligned} P &= (A+B)/2 \\ N &= (A-B)/2 \end{aligned} \tag{10}$$

and

$$\begin{aligned} A &= P+N \\ B &= P-N \end{aligned} \tag{11}$$

This duality, along with some simple trigometric identities, are useful in quantifying many of the imaging non-idealities.

2.3 Hilbert Transforms and Positive-Pass Filters

One of the most important transformations in realizing complex signal processing systems is that of a *positive-pass filter* (PPF). This is a filter that can take a possibly complex input signal[3] and produces a necessarily complex output signal that has positive frequency components only. A signal with positive-frequency components only is called an *Analytic Signal*. It has the property that for every real spectral component, there is a corresponding imaginary spectral component that is equal in magnitude but *delayed in time* by $90°$ [1]. A complex SFG of a system that produces analytic signals from possibly complex signals is shown in Fig. 7. (a) and the equivalent real SFG is shown in Fig. 7. (b). As shown, Hilbert Transform filters are required to produce the time-delay $90°$. For negative frequencies, which have phases continually changing more negative,

3. Most texts [5] only consider the special case of real input signals.

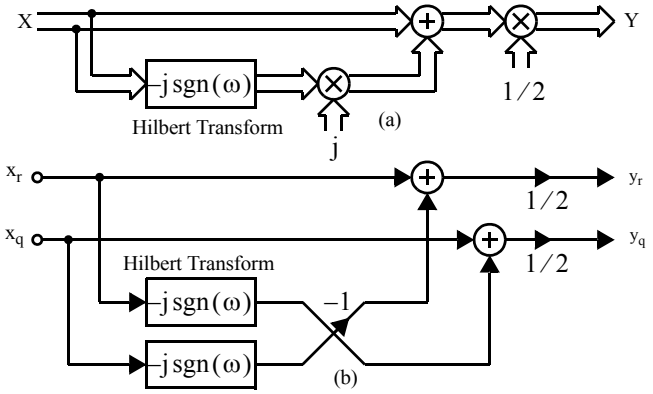

Fig. 7. One possibility for realizing a positive-pass filter (PPF): (a) a complex SFG and (b) an equivalent real SFG.

this means the outputs are phase shifted by $+90°$ as opposed to $-90°$ for positive frequencies which have increasing phases[4]. In a generalization, one is led to complex filters which have passbands at positive frequencies only for a PPF (negative frequencies only for a NPF). These are discussed in Section 4.

3. Complex Modulation and Classical Wireless Systems

We have already seen in the Introduction that a real input signal can be frequency shifted without imaging errors using two real multipliers. This operation frequency shifts both positive and negative frequency components in the same direction by the same amount. This operation, when combined with an appropriate low-pass filter can be used to frequency demodulate an RF input to a complex IF frequency or directly to base-band [12][13][14].

3.1 Direct-Conversion Receiver

The direct-conversion receiver is a good choice of architecture for less demanding, but highly integrated applications [39][40]. A simplified receiver architecture is shown in Fig. 8. using both a complex SFG (Fig. 8. (a)) and a real SFG (Fig. 8. (c)). Example spectra of various locations of Fig. 8. (a) are shown in Fig. 8. (b).

3.2 Direct-Conversion Transmitter

In a direct-conversion transmitter, a complex input signal is directly modulated to RF using a complex mixer, and then converted to a real RF signal by simply ignoring the imaginary output of the complex mixer; this allows us to simplify the complex mixer to two real multipliers as shown in Fig. 9. (c).

3.3 Single-Side-Band (SSB) Generation

One of the first uses of complex processing was for SSB generation. For example, consider the Weaver architecture as shown in Fig. 10.[5] In this approach, the base-band signal, which is symmetric about dc, is frequency shifted up so it is centered at ω_1. The lower sideband is then extracted using two

4. This is inherent in the conjugate-symmetry property of real transfer functions.

5. This is a good example of how complex SFG's can be used to describe systems without using equations.

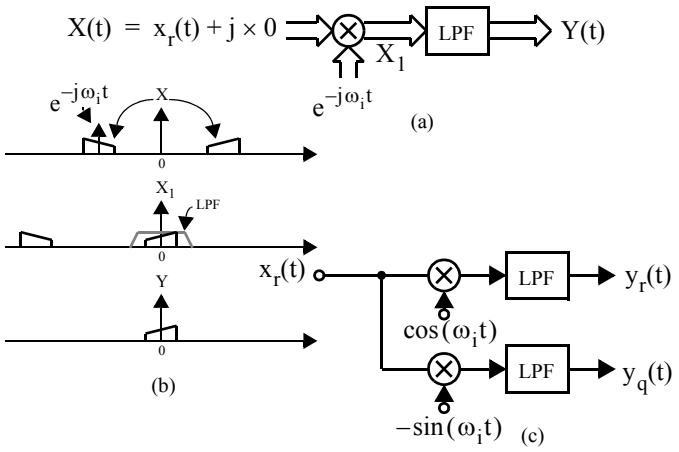

Fig. 8. An image-reject down-converter. (a) The complex SFG, (b) example spectra, and (c) an equivalent real SFG.

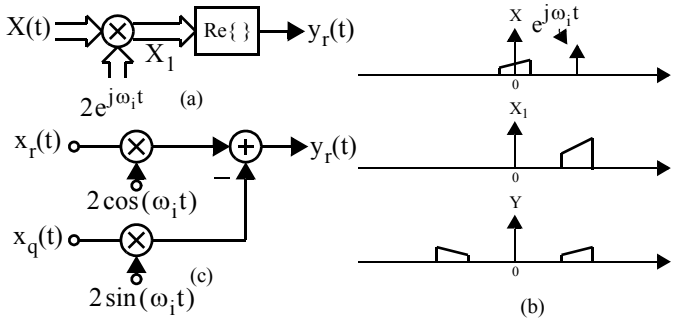

Fig. 9. An image-reject up-converter. (a) The complex SFG, (b) example spectra, and (c) an equivalent real SFG.

real lowpass filters. The complex signal is then further frequency shifted to the desired RF frequency, in this case ω_2, and the imaginary part is discarded resulting in the final SSB signal at RF. The spectra of various locations of the complex SFG of Fig. 10. (b) are shown in Fig. 10. (c).

An alternative architecture for SSB generation, called Weaver's second method, replaces the first complex mixer and the low-pass filters with a complex PPF (or NPF) to extract the desired side-band directly before frequency shifting to the desired RF frequency.

3.4 SSB Receivers

A closely related architecture to SSB transmitters is an alternative for a SSB receiver based on using a PPF after a complex demodulation from RF. The PPF is used to attenuate images as shown in the real SFG of Fig. 11. (a) and the equivalent complex SFG of Fig. 11. (b)[6]. From the plots of the spectra at different locations of the complex SFG, it is seen that the first complex mix frequency shifts the spectra so the only significant components at positive frequencies is the desired side-band. The side-band is extracted using a PPF. The final real demodulated output signal is obtained by simply taking the real output of the PPF and discarding its imaginary output. This approach was originally proposed by Hartley [16] where

6. This is a good example of using complex filtering to eliminate interfering images.

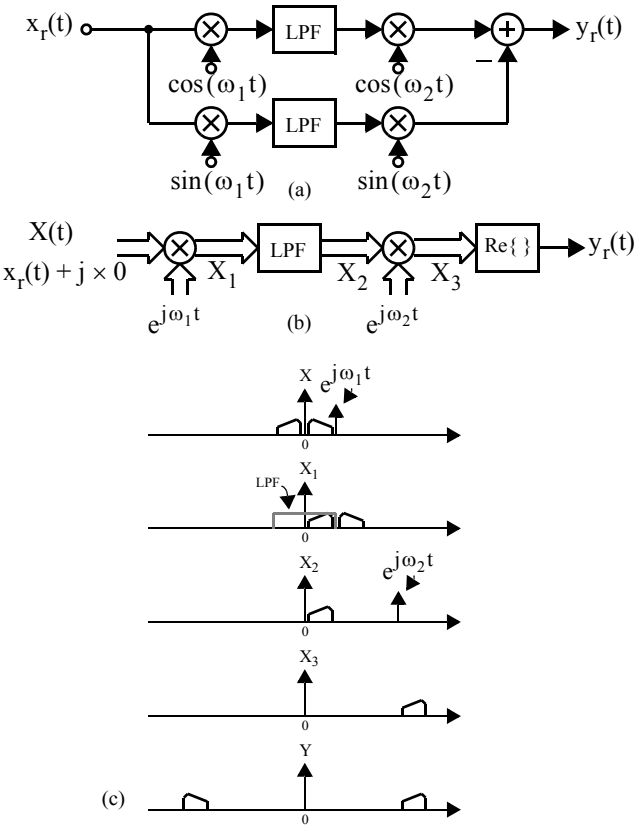

Fig. 10. The Weaver method for SSB generation [15].

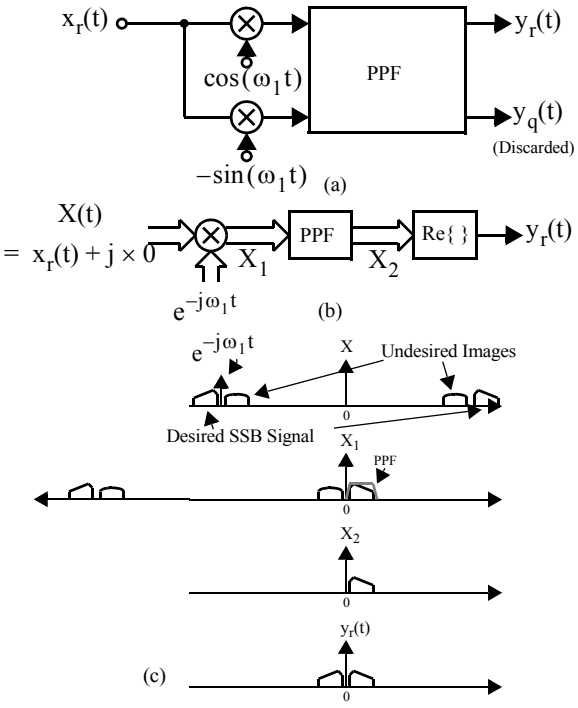

Fig. 11. Demodulating a SSB signal using a Hartley architecture [16].

the PPF was implemented as two low-pass filters cascaded with simple RC phase-shift networks as shown in Fig. 12. (a). An alternative means of realizing a wide-band passive PPF,

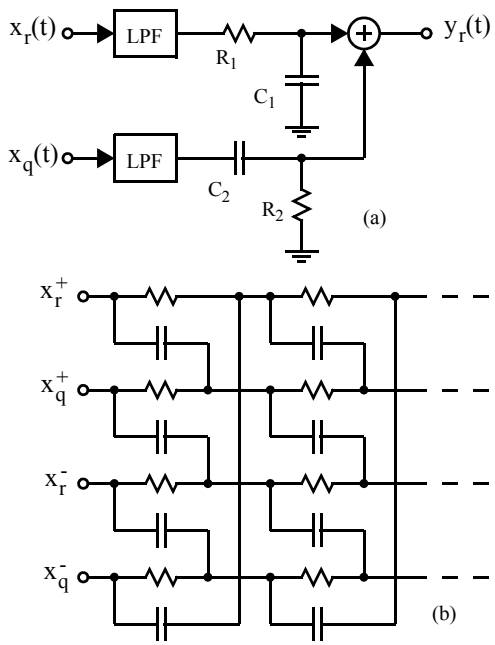

Fig. 12. (a) The PPF used in the Hartley SSB receiver, and (b) the poly-phase approach for realizing a PPF from [17].

that is less sensitive to component tolerances and is currently popular, is the poly-phase network shown in Fig. 12. (b) [17][18][19]. The poly-phase network is well-analyzed in [19] where it is shown that it is an example of a complex filter obtained from frequency-shifting a high-pass filter as is discussed in section 4.

3.5 Imaging Errors in Complex Mixers

Perhaps the major motivation for using image-reject or complex mixers is they allow for frequency translation while minimizing the necessity of highly selective and sensitive image-reject filters at RF and IF frequencies. This is only true to the extent that image-reject mixers operate ideally. For example, if the complexoid that is modulating the input signal has negative frequency components, then interferers can be imaged to fall in band. In addition to errors in the modulating complexoid, gain and phase errors in the two signal paths also cause imaging errors. Assuming these gain and phase errors are wide-band, then they can be modelled assuming error-free signal channels, but additional gain and phase errors in the modulating complexoid. Thus, under this assumption, we only need to quantify wide-band imaging errors due to non-ideal modulating complexoids and not the channels.

Consider the case of demodulating an SSB, but where now the lower side-band is desired for simplicity. This case is similar to that of Fig. 11., but now the ideal demodulating complexoid is at a positive frequency. Assume, it is not ideal; we will show this results in there being a small modulating complexoid at a negative frequency as well, as shown in Fig. 13. (a). The assumed input signal is shown in Fig. 13. (b). The desired frequency shift takes the negative input signal and modulates it so the negative lower side-band is just above dc as shown in Fig.

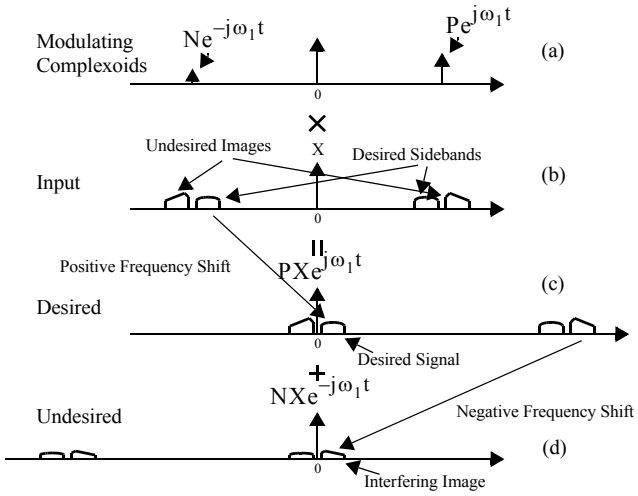

Fig. 13. Imaging due to a non-ideal complexoid.

13. (c). However, the smaller negative modulating complexoid shifts the positive input signals so the upper side-band, although attenuated, is sitting directly at the same frequency band as the desired lower side-band as shown in Fig. 13. (d). The subsequent filtering by the PPF will output both the desired lower side-band and the interfering image. For this reason, it is important to quantify the magnitude of the imaging complexoid (in this case at a negative frequency) as a function of the magnitude and phase errors of the modulating waveform.

Consider an ideal image-reject mixer having a multiplying complexoid given (using rectangular coordinates) as

$$x_{osc}(t) = \cos(\omega_1 t) + j\sin(\omega_1 t) \tag{12}$$

If we assume there are phase and magnitude errors, we can write

$$x_{osc}(t) = \cos(\omega_1 t) + j(1+\varepsilon)\sin(\omega_1 t + \phi) \tag{13}$$

where ε is the magnitude error and ϕ is the phase error. This assumes we have normalized the complexoid so the magnitude of the $\cos(\ )$ term is unity. We can use the well-known trigometric identity

$$\sin(a+b) = \sin(a)\cos(b) + \cos(a)\sin(b) \tag{14}$$

to get

$$\begin{aligned} x_{osc}(t) = {} & [1 + j(1+\varepsilon)\sin\phi]\cos(\omega_1 t) \\ & + j[(1+\varepsilon)\cos\phi]\sin(\omega_1 t) \end{aligned} \tag{15}$$

We can now directly apply (10) to give

$$x_{osc}(t) = Pe^{j\omega_1 t} + Ne^{-j\omega_1 t} \tag{16}$$

where

$$P = \frac{A+B}{2} = \frac{1+(1+\varepsilon)e^{j\phi}}{2} \tag{17}$$

and

$$N = \frac{A-B}{2} = \frac{1-(1+\varepsilon)e^{-j\phi}}{2} \qquad (18)$$

For $\varepsilon, \phi \ll 1$, we see that the positive frequency term is slightly changed in magnitude and phase, these errors are normally small and easy to compensate; however, the negative frequency complexoid, ideally zero, now has a multiplier given by

$$N \cong \frac{1-(1+\varepsilon)(1-j\phi)}{2} \qquad (19)$$

$$\cong -\frac{\varepsilon}{2} + j\frac{\phi}{2}$$

which is also the multiplier for the final resulting images. It might be mentioned that (19) is the basis for a possible adaptive image-reject mixer to be described later.

4. Complex Filters

In addition to image-reject mixers, complex filters are very important and widely-used signal processing blocks in modern wireless transceivers [44]. Complex filters use cross-coupling between the real and imaginary signal paths to realize asymmetrical (in the frequency domain) filters having transfer functions that do not have the conjugate symmetry of real filters. This implies their transfer functions have complex coefficients. The positive-pass filters described previously can be considered a special case of complex filters. Complex filters can be realized using the basic operations of addition, multiplication, and the delay operator for digital filters or the integrator operator for analog filters. Complex analog transfer functions can be realized by either frequency-translating real filters [1][2][10], or by directly deriving transfer complex functions to match asymmetrical specifications using procedures similar to those used for real filters [1][8], and [20]. Similar choices exist for obtaining suitable transfer functions for digital filters [2]-[4],[21]-[25]. In this tutorial introduction, only the real-to-complex transformations will be discussed for reasons of brevity. For the same reason, we will limit our discussions to poly-phase and integrator-based analog filters, and delay-based digital filters.

A complex transfer function can be realized using four real SFG filters [1][12] as shown in Fig. 14. for analog filters. An identical realization is possible for digital filters where the transfer functions are functions of z. For Fig. 14., we have

$$R(s) = \frac{H(s)+H^*(s)}{2} \qquad (20)$$

and

$$jQ(s) = \frac{H(s)-H^*(s)}{2} \qquad (21)$$

When the filters leading from the real and imaginary branches of Fig. 14. do not exactly match, imaging errors (plus less harmful magnitude response errors) occur as we shall see.

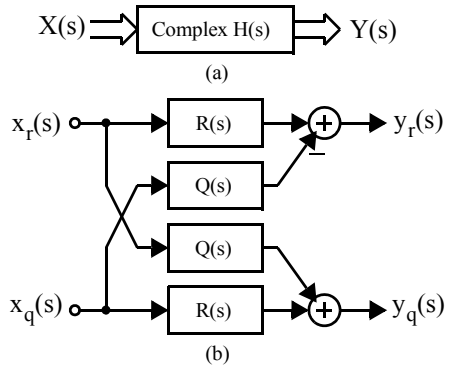

Fig. 14. Realizing a complex filter $H(s) = R(s) + jQ(s)$ *by real SFG transfer filters* $R(s)$ *and* $Q(s)$.

4.1 Frequency-Translated Analog Filters

One method for obtaining complex transfer functions is to do a complex substitution for the Laplace variable s. For example, to effect a positive frequency shift, one uses the substitution

$$s \rightarrow s - j\omega_0 \qquad (22)$$

The effect of this substitution on a low-pass filter is shown in Fig. 15. Thus, one can replace the procedure of realizing a PPF

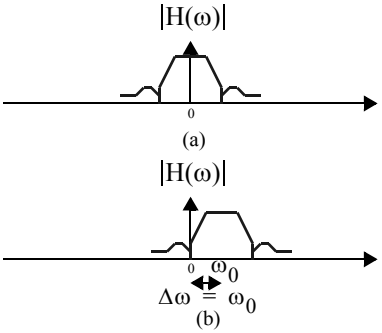

Fig. 15. (a) A base-band prototype magnitude filter response and (b) the magnitude response of a complex filter obtained by the substitution $s \rightarrow s - j\omega_0$.

filter via a Hilbert Transform as shown in Fig. 7. by the more general problem of designing a complex filter that has a pass-band restricted to the desired frequencies, possibly positive only, possibly negative only, or a combination of the two.

An example of using a complex frequency translation is a derivation of a poly-phase network[7]. Consider the passive RC high-pass filter shown in (a). In this example, the transmission zero at dc will be frequency-shifted to negative frequencies, so we use the substitution $s \rightarrow s + j\omega_0$. This transforms the admittance for the capacitor according to

$$sC \rightarrow sC + j\omega_0 C \qquad (23)$$

Letting

7. The derivation presented here is an alternative to that presented in [19].

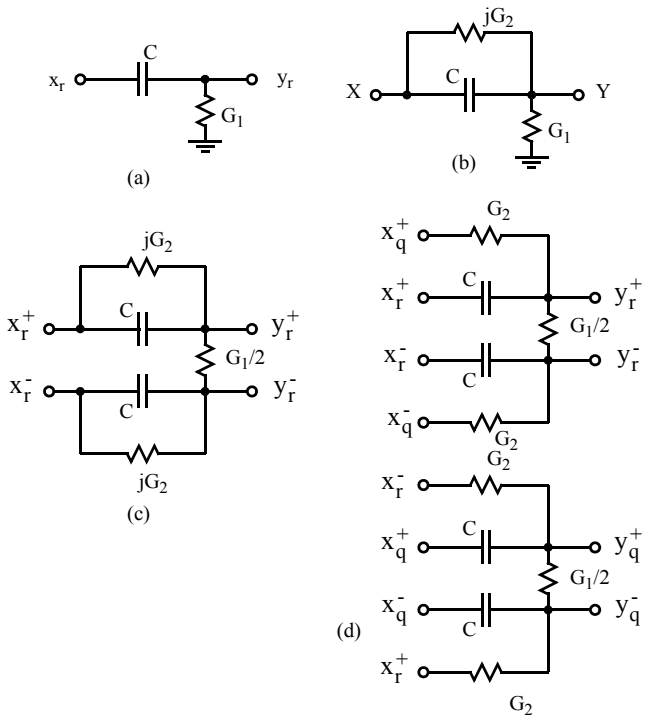

Fig. 16. Using a complex frequency translation to realize a PPF: (a) the high-pass prototype, (b) the complex band-stop having a complex admittance, (c) a fully-differential version of (b), and (d) replacing the complex admittances with cross-coupled real admittances between the real and imaginary paths.

$$\omega_0 = \frac{G_2}{C} \tag{24}$$

gives the required substitution as

$$sC \rightarrow sC + jG_2 \tag{25}$$

Thus, the frequency-shifted high-pass is now as shown in Figure 16 (b). The complex admittance, jG_2, will be realized using cross-coupling between the real and imaginary signal paths. However, the cross-coupling often (from the imaginary to the real signal path) requires inversion (realizing negative components also requires inversion usually); to realize this using passive circuits, fully-differential networks are necessary. A fully-differential version of the circuit of Figure 16 (b) is shown in Figure 16 (c). This can be realized using only real components by a) replicating the circuit for the imaginary path, and b) realizing the complex components using cross-coupling between the two signal paths. Note the input signals to the cross-coupling components going from the imaginary path to the real path are connected from the inverted nodes. The resulting network is shown in Figure 16 (d). Upon examination, this is seen to be identical to the poly-phase network of Figure 12 (b) except for the inclusion of load resistors $G_1/2$ in Figure 16 (d). Taking $G_1 = 0$ would result in very narrow notches. Normally poly-phase networks are intended to be cascaded [17][19] and the load on each section is the succeeding section as discussed in depth in [19].

The procedure just described is general and can be applied to any RC filter whether active or passive to realize a frequency-shifted complex filter.

Alternatively, one can apply a similar procedure for directly frequency-translating SFG filters based on integrators [1]. This procedure is illustrated by applying it to the single integrator shown in Fig. 17. (a). In Fig. 17. (b) and (c) are shown complex

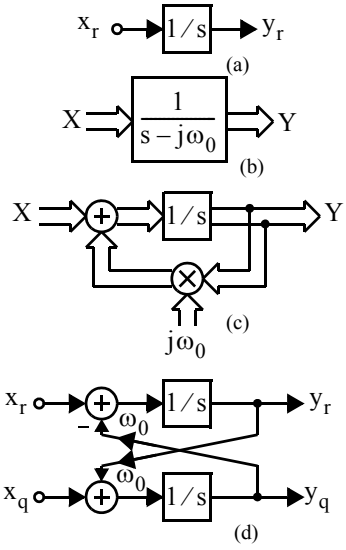

Fig. 17. Frequency shifting a real integrator to a complex positive-frequency integrator.

SFG's that realize the frequency-shifted integrator. The complex SFG of Fig. 17. (c) is converted to the equivalent real SFG of Fig. 17. (d) where the necessary cross-coupling is explicit. The procedure for frequency-shifting any real SFG integrator-based filter is simply: a) replicate the real SFG filter for the imaginary path, and b) cross-couple at each integrator as shown in Fig. 17. (d). As always, this cross-coupling is simplified by using fully-differential circuits.

4.2 Frequency-Translated Digital Filters

Complex discrete-time and digital filters are as essential to modern wireless systems as the complex analog blocks already described. For example, digital complex filters are used as decimation filters for complex A/D's and also as band-limiting filters at base-band for spectral shaping. A similar approach can be used for frequency shifting real discrete-time delay-based digital filters to complex asymmetrical filters [2] as was used for analog filters. Consider the real delay operator

$$z^{-1} = e^{-j\omega T} \tag{26}$$

being frequency shifted by applying the substitution

$$\omega \rightarrow \omega - \omega_0 \tag{27}$$

We have

$$e^{-j\omega T} \rightarrow e^{-j(\omega - \omega_0)T} = z^{-1} e^{j\omega_0 T} \tag{28}$$

Thus, discrete-time filters can be transformed by once again replicating the filter for the imaginary path and then placing a complex-coefficient multiplier directly after every delay operator as shown in Fig. 18. It is obvious that this approach can be

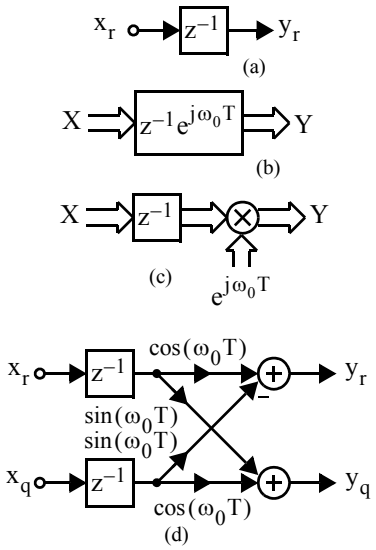

Fig. 18. Frequency shifting a real delay operator to a complex positive-frequency.

used to realize complex filters that have their frequency-shifts programmable. As an additional note, the complex rotation implied by the multiplication by $e^{j\omega_0 T}$ is called a *Cordic* operation and its realization has been well studied [26][27].

Some special cases of frequency-shifted discrete-time filters are worth mentioning. For example, some discrete-time filters are based on using as fundamental building blocks *forward* and *backward-difference integrators*; these are bases for many switched-capacitor (SC) filters realizations. The filters before frequency translation have unity-gain feedback around the delay operators. After translation, it is desirable to preserve this unity-gain feedback to facilitate their realization using SC integrators. This is possible as shown in the original and transformed discrete-time integrators of Fig. 19. Realizing the complex SFG's of Fig. 19. (b) and Fig. 19. (d) using real SFG's is straightforward.

Another interesting special case is a frequency shift by $\pm 1/4$ times the sampling frequency. For this case, we have

$$e^{j\omega_0 T} = e^{\pm j} = \pm j \tag{1}$$

and using Fig. 4., we see that we need only interchange signal paths (and invert one of the paths); this leads to simplified implementations for this popular choice.

4.3 Imaging Errors in Complex Multipliers and Transfer Functions

The analysis of imaging errors due to real coefficient errors in complex multipliers and transfer functions is similar to that presented in Section 3.5 for complex mixers. Consider a generalized multiplication function as shown in Fig. 20. (a) and (b). Assuming

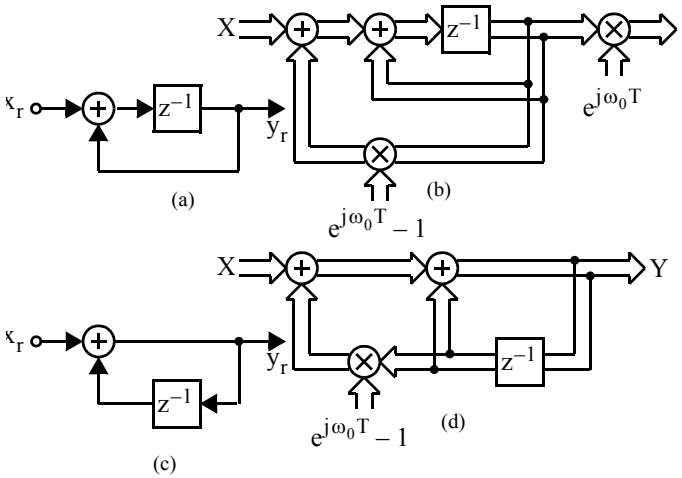

Fig. 19. Frequency-translating (a) the forward-difference integrator and (c) the backward-difference integrators to complex discrete-time integrators.

$$P = \frac{a_1 + a_2}{2} + j\frac{a_1 + a_2}{2} \tag{29}$$

and

$$N = \frac{a_1 - a_2}{2} + j\frac{b_1 - b_2}{2} \tag{30}$$

then it is straightforward to show Fig. 20. (b) is equivalent to Fig. 20. (a). Using (6) and (7), we see that real coefficients errors result in shifting positive frequencies to negative frequencies, and vice versa, with the magnitude of these imaging errors being proportional to the differences of the real coefficients. For example, in-band signal components can be shifted into the stopband. Also, out-off-band interferers can be shifted into the pass-band. If these coefficients errors occur at multipliers inside digital filters, then at the output of each non-ideal multiplier, these imaging components are generated. The imaging components are multiplied by the transfer functions from the multiplier outputs to the filter outputs and subsequently appear as imaging errors at the filter output. To minimize signal-to-stopband errors, one should design to have out-of-band notches in the transfer function from the multiplier output to the filter output [29]. In addition, to minimize interferer to signal errors, one should design to have out-of-band notches in the transfer function from the filter input to the input of the multiplier. These situations can be quantified using the intermediate-function analysis approach described in [1].

A similar situation occurs when realizing complex filters using the approach of Fig. 14. (b) where we now have non-matched filters $R_1(s)$, $R_2(s)$, $Q_1(s)$, and $Q_2(s)$. The non-translated frequency components are filtered by the *average* transfer functions

$$H_{avg}(s) = \frac{R_1(s) + R_2(s)}{2} + j\frac{Q_1(s) + Q_2(s)}{2} \tag{31}$$

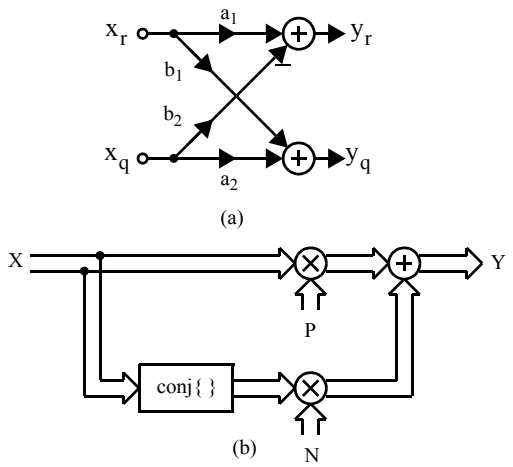

Fig. 20. (a) A generalized multiplication where a_1 , b_1 *are not necessarily equal to* a_2 , b_2 , *and (b) an equivalent complex SFG.*

whereas imaging components are produced (both in-band and out-of-band) by first *conjugating* the input signals, which changes the signs of the frequencies of the spectral components, and then filtering these images by the difference transfer function [1].

$$H_{diff}(s) = \frac{R_1(s) - R_2(s)}{2} + j\frac{Q_1(s) - Q_2(s)}{2} \qquad (32)$$

In this case, the images occur directly at the filter outputs and there is less freedom to minimize images by careful choice of the intermediate transfer functions as compared to when filters are cross-coupled internally.

5. Recent Wireless Applications of Complex Signal Processing

5.1 Adaptive image reject mixers

Many recent wireless receivers tune or adapt the systems to eliminate image errors due to non-ideal image-reject mixers. This tuning can be done in either the analog or the digital domain.

As a preliminary to discussing adaptive algorithms, note that most adaptive systems require the output of a sensitivity filter, $s(t)$, which is correlated with is an error $e(t)$ to drive the error to zero. A possible update algorithm is given by

$$\Delta k_i = -\mu \langle e, s \rangle \qquad (33)$$

where μ is a small constant controlling the update rate. Often this update is approximated using the stochastic instantaneous update to give

$$k_i(n) = k_i(n-1) - \mu e(n) s^*(n) \qquad (34)$$

Note that $s^*(n)$ *is conjugated*. Alternatively, $e(n)$ could have been conjugated. The required sensitivity filter, $s(n)$ is often trivial for FIR systems, and often not too complicated even for IIR systems [30][31] (and can be found using Tellegen's Theorem [5]).

A possible approach to adapt an image-reject mixer is based on (19). In this approach, assume a complex mixer is used to demodulate an RF signal to a low IF. A complex PPF can be used to extract the desired signal. In addition, assume a NPF is used to extract the undesired signal-induced image at negative frequencies. If the PPF and NPF complex outputs are multiplied together, then the approximate result is a complex dc signal given by (19). Thus, the real output of the multiplication can be used to drive the gain error to zero, and the imaginary part can be used to drive the phase errors to zero. This assumes the errors are frequency-independent. In normal practice, the signal processing would be done in the digital domain, but the tuning would be done in the analog domain at the multipliers. This approach can suffer from biases due to interferers. The approach just proposed is similar to that described in [32], except in [32] the adaptation was done with an interferer only used as a reference input, the error functions minimized are different, and the adaptation update was performed in the analog domain.

Alternative improved approach, where the signal processing and the tuning are both done in the digital domain, are described in [33][34], with a realization based on [34] described in [35]. The approach is shown in Fig. 21. As in the

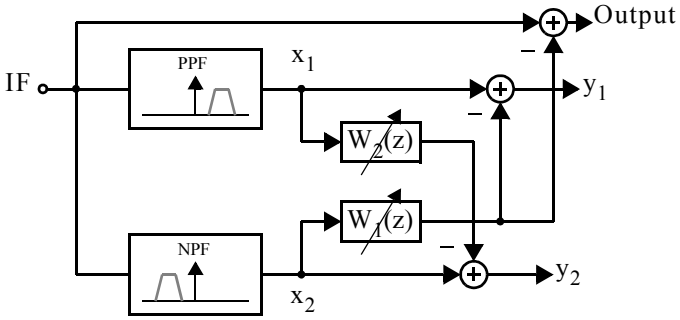

Fig. 21. A digital adaptive filter approach for adapting an image-reject mixer.

previous approach a complex PPF is used to extract the desired signal, and a second NPF is used to extract the images. An improvement of this approach is that a symmetric decorrelating filter is used to minimize image components in y_1 and signal components in y_2 [36]. This helps minimize biases. Another advantage of this approach is *frequency-dependent* imaging errors are cancelled as well. It is speculated that the decorrelating technique could also be applied to improve the previous algorithm. A recently proposed algorithm [37], although completely implemented in the digital domain, does include some features of both of the above algorithms. Another interesting adaptive image-reject approach that again is completely in the digital domain is based on blind source separation compensation [38].

The alternatives just described are just the beginning of what is expected to be a fruitful area of research. One future possibility is to tune in both the analog and the digital domain. Tuning the mixer inputs in the analog domain is useful in

preventing overload in the IF stages and to help attain timing acquisition, but is only useful for correcting frequency-independent errors. A second adaptive fine-tuning in the digital domain similar to [34] can be used to further eliminate frequency-dependent errors of, for-example, complex over-sampling A/D's used at the IF.

5.2 Low-IF Receivers.

A currently popular architecture for realizing highly-integrated moderately wide-band wireless transceivers is the low-IF architecture [41][42][43]. An example of a low-IF receiver is shown in Fig. 22. In a low-IF receiver, the RF signal

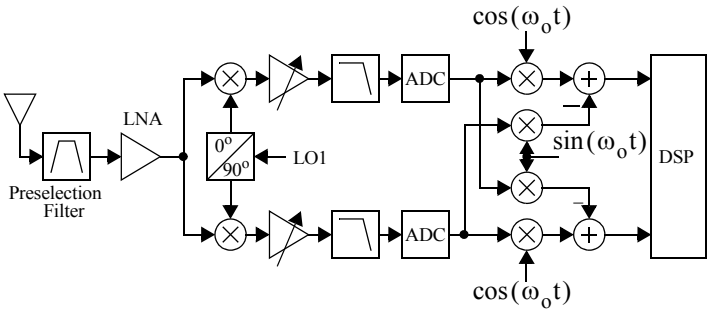

Fig. 22. A low-IF architecture for a receiver.

is demodulated in two stages; the first stage is a standard image-reject mixer which requires two analog real multipliers. This translates the RF input signal down to a low-IF frequency, after which a second complex mixer is used to shift the IF signal to base-band. The second complex mixer requires four real multipliers. These can be realized using analog multipliers as in [42]. Alternatively, the A/D conversion can be done at the IF stage as shown in Fig. 22., and then the second complex frequency shift can be realized in the digital domain [43]. This allows the second complex modulation to be almost ideal. Also, if the A/D sampling frequency is chosen to be a small multiple of the IF frequency, then the second mix is significantly simplified. For example, if the sampling frequency is four times the IF frequency, then the oscillator inputs to the second complex digital mixer are ± 1 or 0. This digital modulation alternative is often preferable.

Low-IF architectures are especially suitable for multi-standard receivers when the channel-selection filters are realized after the A/D converters using digital circuits, and, thus, can be programmed to accommodate the requirements of the different standards. The low-IF architectures greatly minimize errors due to feedback of the local-oscillator (LO) and the large 1/f noise of MOS transistors. They do suffer from images when the IF frequency is low, but these can be significantly minimized by using even relatively simple complex filters at the IF [44].

In general, when the A/D conversion occurs before the channel-selection filters, then the A/D conversion must necessarily be high dynamic range, and *the A/D converter is almost always the limiting factor determining the maximum achievable data rate of the receiver.* Assuming the A/D converter is the limiting factor on the maximum achievable data rate, then it is possible to double the maximum-achievable data rate using the modulation approach proposed in [45]. A typical low-IF architecture has IF spectral components at positive or negative frequencies only; this wastes half the available bandwidth of the A/D's[8]. It is possible to send additional data in the unused frequency band. In the simplest implementation, one channel is implemented at positive frequencies and one channel is implemented at negative frequencies; in more-advanced realizations, multiple channels are implemented at both positive and negative frequencies using orthogonal-frequency-division-multiplexing (OFDM) techniques. In both cases the physical hardware is the same as for typical low-IF receivers (as shown in Fig. 22.); the increase in complexity is all in the digital domain and is quite feasible.

The approach for single channels only at positive and negative frequencies is shown in Fig. 23. At the transmitter, two

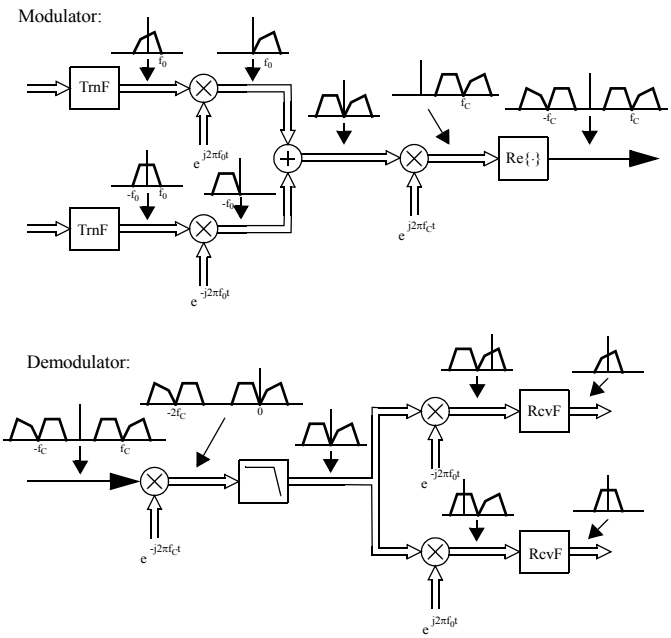

Fig. 23. A Hierarchical Modulation approach to achieve twice the data rate for a given sampling rate of the A/D's.

quadrature input channels are used; one is modulated to positive frequencies, and one is modulated to negative frequencies. A guard-band is left at dc. The congregate is modulated up to the RF and transmitted. This approach is much like a double single-side-band system where both an upper and a lower side-band are transmitted together. At the receiver, the RF signal is demodulated so one channel is again at a positive IF and the second channel is at a negative IF. The guard-band at dc allows the IF signal to be ac coupled which eliminates errors due to the local feedback of the RF oscillator and 1/f noise. The IF signal is then digitized similar to a typical low-IF architecture. After the A/D conversion, the individual channels can be

8. This assumes the A/D converters are not complex over-sampling A/D's; if they are, the bandwidth is not necessarily wasted. This is one of the motivations for using complex over-sampling A/D's.

independently demodulated as shown in Fig. 23. using complex signal processing in the digital domain

5.3 Complex and Quadrature Over-sampling A/D Converters

All signal processing blocks preceding the channel-selection filters in a receiver must be high dynamic range. Typical specifications are linearities equivalent to 14-bit ideal A/D converters or more (86 dB SNDR or more). Typical specifications for the analog bandwidths are now in excess of 2MHz and as high as 5MHz. Realizing A/D converters that can meet these demanding specifications is a challenging task. A possible architecture that is gaining in popularity is the complex over-sampling A/D converter. Complex over-sampling ΔΣ A/D converters (invented by W.M Snelgrove and S. Jantzi) combine the complex filtering ideas of [1] and the real bandpass over-sampling ΔΣ A/D converters of [46]. By using a complex filter in the ΔΣ loop, the effective signal bandwidth is cut in half which doubles the over-sampling-ratio (OSR) giving ideally a much-improved SNDR [47][48] depending on the order of the over-sampling loop and the resolution of the D/A's included in it. Also, it is possible to choose the locations of the zeros of the noise-transfer function (NTF) to minimize errors due to quantization effects, and, finally, the zeros of the signal-transfer function (STF) can be independently chosen to filter out images from an imperfect preceding image-reject mixer, effectively combining complex image-reject filtering and the A/D conversion in a single unit. The basic architecture of the complex over-sampling ΔΣ A/D converter is shown in Fig. 24.

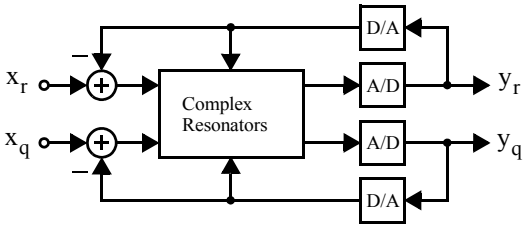

Fig. 24. A complex ΔΣ over-sampling A/D converter architecture.

In [48], a 4'th order (complex — 8'th order real) complex over-sampling A/D was reported which used 1-bit internal converters. A complex SFG of the architecture showing the complex resonators is shown in Fig. 25. It should be noted that each

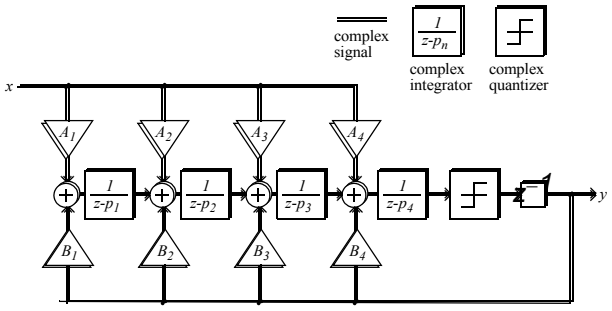

Fig. 25. Complex SFG of fourth-order quadrature ΔΣ modulator from [48].

of the p_i coefficients are complex. The design of the internal complex resonator-based filter was done to maximize SNDR by careful choice of the noise-transfer function (NTF) and signal-transfer function (STF) transmission zeros [29]. The converter was implemented using switched-capacitor (SC) circuits. A single-ended version of the converter is shown in Fig. 26. This first integrated quadrature ΔΣ converter had

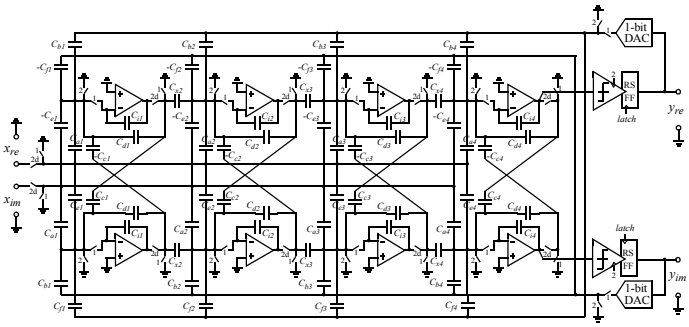

Fig. 26. A single-ended SC realization of the ΔΣ converter of Fig. 25.

measured SNDR of 65 dB for a 100kHz signal bandwidth. It was also found to have better stability properties than real over-sampling converters. Recently, there have been examples of continuous-time complex ΔΣ A/D converters reported as well [49][50]. For example, the converter reported in [50] exhibited an SNDR of 76 dB for a 1MHz signal bandwidth, yet dissipated just 4.4mW. These are excellent results.

Currently, there has been little published on how to best implement the complex digital filters required for decimation after the analog modulators to eliminate quantization noise. This is expected to be an active area for future research.

6. Conclusion

A tutorial description of the use of complex signal processing in wireless systems has been presented. First, the fundamentals have been explained and then their use in a number of applications has been described. Throughout, a highly-graphical signal-flow-graph approach has been used. The applications of complex mixers, filters, low-IF receivers, and A/D converters have been emphasized.

7. References

[1] W. M. Snelgrove, *Intermediate Function Synthesis*, Ph.D. Thesis, University of Toronto, 1982.

[2] T. H. Crystal and L Ehrman, "The Design and Applications of Digital Filters with Complex Coefficients," *IEEE Trans. Audio and Electroacoustics*, AU-16, No. 3, pp. 315-320, Sept. 1968.

[3] R. Boite and H. Leich, "On Digital Filters with Complex Coefficients," in *Network and Signal Theory* (edited by J.K. Skwirzynski and J.O. Scanlan), pp. 344-351, Peter Peregrinus, London, 1973.

[4] M.T. McCallig, "Design of Digital FIR Filters with Complex Conjugate Pulse Responses," *IEEE Trans. on Circuits and Systems,* CAS-25, pp. 1103-1105, Dec. 1978.

[5] A.V. Oppenheim and R.W. Schafer, *Digital Signal Processing*, Prentice-Hall, 1975.

[6] W.M. Snelgrove and A.S. Sedra, "State-Space Synthesis of Complex Analog Filters," in *Proc. of the European Conference on Circuit Theory and Design*, pp. 420-424, 1981.

[7] G. R. Lang and P.O. Brackett, "Complex Analogue Filters," in *Proc. of the*

European Conference on Circuit Theory and Design, pp. 412-419, 1981.
[8] W.M. Snelgrove, A.S. Sedra, G.R. Lang, and P.O. Brackett, "Complex Analog Filters," 1981, ftp://ftp.eecg.toronto.edu/pub/software/martin/snelgrove_cmplx.pdf.
[9] R. Allen, "Complex Analog Filters Obtained from Shifted Lowpass Prototypes," M.A.Sc. Thesis, University of Toronto, 1985.
[10] A. Sedra, W. Snelgrove, and R. Allen, "Complex Analog Bandpass Filters Designed by Linearly Shifting Real Low-Pass Prototypes," in *Proc. of Int. Symp. on Circuits and Systems,* Vol. III, pp. 1223-1226, 1985.
[11] Q. Liu, "Switched-Capacitor Complex Filters," M.A.Sc. Thesis, University of Toronto, 1985.
[12] E.A. Lee and D.G. Messerschmitt, *Digital Communication*, Kluwer Academics Publishers, Boston, 1988.
[13] J. Crols and M. Steyaert, *CMOS Wireless Transceiver Design*, Kluwer Academics Publishers, Boston, 1997.
[14] B. Razavi, *RF Microelectronics*, Prentice Hall, NJ, 1998.
[15] D. K. Weaver, Jr., "A Third Method of Generation and Detection of Single-Sideband Signals," *Proc. IRE*, pp. 1703-1705, June 1956.
[16] R. Hartley, "Modulation System," U.S. Patent 1666206 Apr. 1928.
[17] M. J. Gingell, "Single-Sideband Modulation Using Sequence Asymmetric Polyphase Networks," *Electrical Communication,* Vol. 48, No. 1-2, pp. 21-25, 1973.
[18] J. Crols and M. Steyaert, "An Analog Integrated Polyphase Filter for a High-Performance Low-IF Receiver," *Proc. VLSI Circuits Symposium*, Kyoto, pp. 87-88, June. 1995.
[19] F. Behbahani, Y. Kishigami, J. Leete, A. Abidi, "CMOS Mixers and Polyphase Filters for Large Image Rejection," *IEEE J. of Solid-State Circuits,* Vol. 36, No. 6, June 2001.
[20] C. Cuypers, N. Voo, M. Teplechuk, and J. Sewell, "The General Synthesis of Complex Analogue Filters," 9'th Intl. Conf. on Elect., Circuits, and Systems, Vol. 1, pp. 153-156, 2002.
[21] A. Fettweis, "Principles of Complex Wave Digital Filters," *Int. J. Circuit Theory Appl.*, Vol. 9, pp. 119-134, Apr. 1981.
[22] X. Chen and T.W. Parks, "Design of FIR Filters in the Complex Domain,: *IEEE Trans. on Acoustics, Speech, and Signal Processing*, Vol. 35, No. 2, pp. 144-153, Feb. 1987.
[23] P. Regalia, S. Mitra, and J. Fadavi-Ardekani, "Implementation of Real Coefficient Digital Filters Using Complex Arithmetic, *IEEE Transaction on Circuits and Systems,* Vol. CAS-34, No. 4, pp. 345-353, Apr. 1987.
[24] X. Chen and T. Parks, "Design of IIR Filters in the Complex Domain, "*IEEE Trans. on Acoustics, Speech, and Signal Processing*, Vol. 38, No. 6, pp. 910-920, Jun. 1990.
[25] M. Komodromos, S. Russell, and P.T.P. Tang, "Design of FIR Filters with Complex Desired Frequency Response Using a Generalized Remez Algorithm," *IEEE Transactions on Circuits and Systems-II*, vol. 42, no. 4, pp. 428-435, Apr. 1995.
[26] J. Volder, "The CORDIC Trigometric Computing Technique," *IEEE Trans. on Computers,* Vol. EC-8, pp. 330-334, Sept. 1959.
[27] A. Madisetti, A. Kwentus, and A.N. Willson, Jr., "A 100-MHz 16-b Direct Digital Frequency Synthesizer with a 100-dBc Spurious-Free Dynamic Range, *IEEE Journal of Solid-State Circuits*, vol. 34, no. 8, pp. 1399-1410, Aug. 1999.
[28] K.W. Martin, "Small Side-Lobe Filter Design for Data Communication Applications," *IEEE Transactions on Circuits and Systems-II*, vol. 45, no. 8, pp. 1155-1161, Aug. 1998.
[29] S. Jantzi, K. Martin, and A.S. Sedra, "The effects of Mismatch in Complex Bandpass $\Sigma\Delta$ Modulators," *Proc. IEEE Intl. Symp. on Circuits and Systems (ISCAS)*, pp. 227-230, May 1996.
[30] K. Martin and M.T. Sun, "Adaptive Filters Suitable for Real-Time Spectral Analysis," *IEEE Trans. on Circuits and Systems*, Vol. CAS-33, No. 2, pp. 218-229, Feb. 1986.
[31] T. Kwan and K. Martin, "Adaptive Detection and Enhancement of Multiple Sinusoids Using a Cascade IIR Filter," *IEEE Trans. on Circuits and Systems*, Vol. CAS-36, No. 7, pp. 937-947, July 1989.
[32] L. Der and B. Razavi, "A 2-GHz CMOS Image-Reject Receiver with LMS Calibration," *IEEE Journal of Solid-State Circuits*, Vol. 38, No. 2, pp. 167-175, Feb. 2003.
[33] J. Paez-Borrallo, and F.J. Casajus Quiros, "Self adjusting digital image rejection receiver for mobile communications," *IEEE Vehicular Technology Conference*, Vol. 2, pp. 686 -690, May 1997
[34] L. Yu and W.M. Snelgrove, "A Novel Adaptive Mismatch Cancellation System for Quadrature IF Radio Receivers, *IEEE Transactions on Circuits and Systems-II*, vol. 46, no. 6, pp. 789-801, Jun. 1999.
[35] K. Pun, J. Franca, and C. Azeredo-Leme, "The Correction of Frequency-Dependent I/Q Mismatches in Quadrature Receivers by Adaptive Signal Separation," *Proc. IEEE Intl. Symp. on Circuits and Systems (ISCAS)*, pp. 424-427, 2001.
[36] D.V. Compernolle, and S.V. Gerven, "Signal Separation in a Symmetric Adaptive Noise Canceler by Output Decorrelation," *IEEE Trans. Signal Processing,* Vol. 43. pp. 1602-1612, July 1995.
[37] C.C. Chen and C.C. Huang, "On the Architecture and Performance of a Hybrid Image Rejection Receiver, *IEEE J. on Selected Areas in Communications,* Vol. 19, No. 6, pp. 1029-1040, Jun. 2001.
[38] M. Valkama and M. Renfors, "Advanced Methods for I/Q Imbalance Compensation in Communication Receivers," *IEEE Trans. on Signal Proc., Vol. 49, No. 10., pp. 2335-2334, Oct. 2001.*
[39] A.A. Abidi, "Direct-Conversion Radio Transceivers for Digital Communications," *IEEE Journal of Solid-State Circuits*, vol. 30, no. 12, 1995, pp. 1399-1410.
[40] B. Razavi, "Design Considerations for Direct-Conversion Receivers," *IEEE Transactions on Circuits and Systems-II*, vol. 44, No. 6, pp. 428-435, 1997.
[41] J. Crols and M.S.J. Steyaert, "A Single-Chip 900 MHz CMOS Receiver Front-End with a High Performance Low-IF Topology," *IEEE Journal of Solid-State Circuits*, Vol. 30, No. 12, pp. 1483-1492, Dec. 1995.
[42] J.C. Rudell, J. Ou, T.B. Cho, G. Chien, F. Brianti, J.A. Weldon, and P.R. Gray, "A 1.9-GHz Wide-Band IF Double Conversion CMOS Receiver for Cordless Telephone Applications," *IEEE Journal of Solid-State Circuits*, Vol. 32, No. 12, pp. 2071-2088., Dec. 1997.
[43] J. Crols and M. Steyaert, "Low-IF Topologies for High-Performance Analog Front Ends of Fully Integrated Receivers," *IEEE Transactions on Circuits and Systems-II*, vol. 45, no. 3, pp. 269-282, Mar. 1998.
[44] P. Kong-pang, J.E. Franca, C. Azeredo-Leme, "A Quadrature Sampling Scheme with Improved Image Rejection for Complex-IF Receivers," *Proc. IEEE Intl. Symp. on Circuits and Systems (ISCAS)*, pp. 45-48, May 2001.
[45] S. Mirabbasi and K. Martin, "Hierarchical QAM: A Spectrally Efficient DC-Free Modulation Scheme," *IEEE Communications Magazine*, Vol. 38, No. 11, pp. 140-146, November 2000.
[46] S.A. Jantzi, W.M. Snelgrove, and P.F. Ferguson, Jr., "A Fourth-Order Bandpass Sigma-Delta Modulator," *IEEE Journal of Solid-State Circuits*, Vol. 28, pp. 282-291, Mar. 1993.
[47] S. Jantzi, "Quadrature Bandpass Delta-Sigma Modulation for Digital Radio," Ph.D. Thesis, University of Toronto, 1997.
[48] S.A. Jantzi, K. Martin, and A.S. Sedra, "Quadrature Bandpass $\Delta\Sigma$ Modulation for Digital Radio," *IEEE Journal of Solid-State Circuits*, Vol. 32, No. 12, pp. 1935-1949, Dec. 1997.
[49] F. Henkel, et al., "A 1MHz-Bandwidth Second-Order Continuous-Time Quadrature Bandpass Sigma-Delta Modulator for Low-IF Receivers, *IEEE ISSCC*, pp. 214-215, Feb. 2002.
[50] K. Philips, "A 4.4mW 76dB Complex $\Sigma\Delta$ ADC for Bluetooth Receivers, *IEEE ISSCC*, pp. 64-65, Feb. 2003.